THE DESIGN, ANALYSIS, AND TESTING OF A LOW-BUDGET WIND-TUNNEL FLUTTER MODEL WITH ACTIVE AERODYNAMIC CONTROLS*

R. Bolding

Fort Worth Division, General Dynamics Corporation

R. Stearman

The University of Texas at Austin

SUMMARY

Active control technology is playing a more significant role in aerospace and aircraft vehicle design and gives rise to the need to introduce the basic technology into the educational activities within the profession. The present paper describes a low-budget flutter model incorporating active aerodynamic controls for flutter suppression studies, designed as both an educational and a research tool. The study concentrates on the interfering lifting surface flutter phenomenon in the form of a swept wing-tail configuration. A flutter suppression mechanism was first demonstrated on a simple semirigid three-degree-of-freedom flutter model of this configuration employing an active stabilator control. This was then verified analytically using a doublet lattice lifting surface code and the model's measured mass, mode shapes, and frequencies in a flutter analysis. These preliminary studies were significantly encouraging to extend the analysis to the larger degree of freedom AFFDL wing-tail flutter model where additional analytical flutter suppression studies indicated significant gains in flutter margins could be achieved. The analytical and experimental design of a flutter suppression system for the AFFDL model is presented along with the results of a preliminary passive flutter test.

INTRODUCTION

The increased importance that active control technology plays in aircraft and aerospace vehicle design necessitates the introduction of the basic concept into the educational activities within our profession. While the basic technology evolved within the aerospace industries and the government laboratories, certain problem areas appear suitable for pursuit in an academic institution having a combined educational and research objective. The present paper describes one such attempt at a low-budget program carried out at the graduate

*This research was supported by the Air Force Office of Scientific Research, Office of Aerospace Research, United States Air Force.

level. This involved the design, construction, and wind-tunnel testing of an actively controlled wind-tunnel research flutter model. It focused on the development of a flutter suppression system for aerodynamically interfering lifting surfaces in the configuration of a closely spaced wing-tail geometry where the flutter mechanism is fairly well understood.

In early experiments, Topp, Rowe, and Shattuck observed the phenomenon of wing-tail interference flutter for the variable-sweep configuration and indicated in reference 1 that it was the result of aerodynamic interaction and elastic coupling between the wing and tail. For some sweep angles this can significantly reduce the flutter speed for the wing and tail below that for the isolated wing alone as illustrated in figure 1 taken from reference 1. A systematic and extensive study of this phenomenon was carried out by Mykytow, Noll, Huttsell, and Shirk in reference 2 and the wing-tail interference flutter mechanism was fairly well clarified. A small, interesting semirigid flutter model demonstrating this flutter phenomenon was also developed within the industry, as illustrated in reference 3. We later built and adapted this to the classroom demonstration model illustrated in figure 2. As the control configured vehicle and active control concepts further developed, a decision was made to extend the capabilities of this classroom model to demonstrate flutter suppression via active controls. This was undertaken with the hope that the objective could be accomplished, i.e., flutter suppressed over a significant velocity range, and that some insight could also be obtained as to the flutter suppression mechanism. The results of this study proved to be more encouraging than originally anticipated and further analytical studies were carried out on the AFFDL wing-tail flutter model of reference 2 which had several additional flexible degrees of freedom. Here again, parameter optimization techniques yielded control laws which demonstrated significant gains in flutter margin when an active stabilator or aileron control was employed. Flutter margins could be increased to that of the isolated wing. As a result of these analytical findings, it appeared desirable to evaluate the results in the wind tunnel and establish a level of confidence for the math modeling. The present study was undertaken with this objective in mind subject to the constraints of a low budget for model construction and wind-tunnel test time. This necessitated testing at a Mach zero condition in a subsonic wind-tunnel facility. In addition, to cut costs, the existing AFFDL Wind-Tunnel Flutter Model design was selected where minor modifications to the design could be made to yield an active stabilator control. The scope of the experiment was to evaluate control laws derived by parameter optimization techniques employing standard V-g, Vector Nyquist, and aerodynamic energy techniques. The experimental flutter data are to be correlated with analytical flutter calculations based upon lifting surface doublet lattice aerodynamics and experimentally determined mode shapes, generalized masses, and natural frequencies for the first five mode shapes of the system. The flutter suppression system analytical design studies are presented here along with a review of the model design and passive wind-tunnel flutter studies.

The cooperation of the Air Force Flight Dynamics Laboratory (AFFDL) in providing us with the basic model design details is appreciated. In addition, our visits with the Flight Controls staff of the Boeing Company, Wichita Division, were very helpful. Appreciation is also expressed to Emil Cwach,

General Dynamics, Forth Worth, and Lt. Kenneth Griffin, Air Force Flight Dynamics Laboratory, for their contributions to the program.

PRELIMINARY DESIGN STUDIES ON SEMIRIGID MODEL

The actively controlled flutter model, developed in the following program, evolved from preliminary design studies of flutter suppression systems applied to the small semirigid model illustrated in figure 2. At the time the study was initiated it appeared as though a flutter suppression system might be more easily developed for this type of model, that is, it seemed plausible that flutter suppression systems might significantly benefit the performance of variable-geometry aircraft with aerodynamic interference effects while possibly providing less impressive gains on more conventional aircraft. In view of this, exploratory wind-tunnel studies were initiated in the University of Texas 3 ft by 4 ft low-speed wind tunnel with this three-degree-of-freedom model. The degrees of freedom include a rigid body roll mode, one wing bending mode, and one fuselage torsion mode. For the actively controlled model an additional control degree of freedom was incorporated as a stabilator pitch mode. This finite degree of freedom or semirigid feature was achieved by concentrating elastic springs on the model at the wing root and at one position along the fuselage as illustrated by the component breakdown in figure 2.

Trial and error low-speed wind-tunnel tests indicated that a 40% increase in flutter margin could be easily achieved on this model employing a simple feedback coupled to a stabilator control. This was accomplished by taking the output from an accelerometer mounted on the stabilator or fuselage and feeding it through a phase and gain network (or variable phase oscillator) to a small shaker with a force output of 8.9 newtons (2 lb) which activated the stabilator control by means of a flexible mechanical linkage. Interpretation of high-speed movies of the study indicated that the more effective phase and gain selections were those which essentially rotated the stabilator control to eliminate the induced downwash as illustrated in figure 3. This figure represents a view of a typical section cutting through both wing and tail at a given spanwise station. The typical washout appearance of an upward bending swept wing is demonstrated here inducing a downwash over the stabilator forcing it to deform approximately 180° out-of-phase with the wing. The actual phasing will depend upon the wing-tail separation distance. As indicated, the most effective control command for suppressing this interference flutter was that which pitched the stabilator approximately in-phase with the main wing, thus eliminating the induced downwash.

To check the above hypothesis, an analytical study of the model was carried out employing the doublet lattice lifting surface theory and the model's measured mass, mode shapes, and frequencies in a V-g type flutter analysis. The results of this study are illustrated in figures 4 and 5 for the control loop open (passive flutter studies). The experimentally measured flutter speed is superimposed on the V-g data to illustrate the degree of correlation between theory and experiment. A polar plot of the open loop flutter mode in terms of the three generalized coordinates and the motion of a point on the wing and tail are illustrated in figure 5. The actual phasing between the wing and tail

motion is seen to be a little less than the 180° that was suggested. A similar polar plot of the closed loop configuration that suppressed flutter is illustrated in figure 6. This is again based on the doublet lattice aerodynamic modeling now including an active stabilator control and measured modes, frequencies, and model mass. The control deflection, that is, the stabilator pitch, is nearly in-phase with the wing motion which, according to figure 3, eliminates the induced downwash. The wing displacement slightly leads that of the control due to the wing-tail separation distance. An illustration of the gain in flutter margin obtained from both the analytical and experimental models is illustrated in figure 7. For the relatively high damping values (g = 0.05) found for the model structural modes, this represents over a 40% increase in flutter speed. Figure 8 illustrates that the flutter speed could be easily increased by another 50% if the sensor or accelerometer had been placed in a more optimal position such as on the wing instead of the tail.

All these preliminary studies employed an assumed form of control law, originally introduced by Nissim in reference 4, and utilized a parameter optimization procedure to select the control law coefficients which maximized the flutter speed. Details on this analysis can be found in reference 5.

One additional comment is in order concerning the aerodynamic modeling employed in this and the following studies. Both the semirigid and AFFDL model are half-span models; this considerably reduces the model cost and complexity of wind-tunnel installation and testing. These simplifying gains, however, result in the assumption that the model fuselage (in the semirigid case) and the wind-tunnel wall in the AFFDL configuration represents a reflecting plane through which no flow penetrates. In the lifting surface codes employed for the flutter analysis, this requires a symmetric mode input option into the study since the image system is performing a symmetric motion to satisfy the flow boundary condition. This should not lead to any serious problems since no attempt is made here to model a specific configuration where the actual wing-tail flutter mode is found to be antisymmetric.

ANALYTICAL DESIGN STUDIES ON AN ACTIVELY CONTROLLED AFFDL WING-TAIL FLUTTER MODEL

On the basis of the preliminary findings from the semirigid wing-tail model, further analysis seemed justified on a more complex flutter model of similar configuration. The AFFDL wing-tail flutter model had been extensively studied in the wind tunnel and its passive flutter characteristics well documented in reference 2. It was therefore chosen as the best candidate for further investigation. A flutter suppression design based upon optimal control principles and an approximate transient aerodynamic analysis was rejected as being too complex for the present study. Instead a frequency domain design analysis was carried out where the coefficients in an assumed form of control law were determined by parameter optimization procedures. The design study employed the standard V-g method of flutter analysis as well as the aerodynamic energy and Vector Nyquist concepts. Following the work of Nissim in reference 4, an assumed feedback control law was taken of the form

$$\{\delta\} = [C_R + iC_I]\ \{q\} = [C]\ \{q\} \tag{1}$$

where $\{\delta\}$ is a vector representing the displacements of the active aerodynamic control surfaces; $\{q\}$, the complex vector of generalized coordinates defining the motion of the main lifting surfaces; and $[C_R + iC_I]$, a complex matrix relating the motion of the main lifting surfaces to that of the control surfaces. The [C] matrix is the assumed form of feedback control law and its elements may be a function of the frequency or reduced frequency of motion as well as other parameters defining the flight envelope. This assumed feedback control law also implies that all the system generalized coordinates must be observed. This is not practical or even necessary in most cases. Consequently the outputs from a discrete set of motion sensors are related to the generalized coordinates defining the system motion by

$$\{Z\} = [F]\ \{q\} \tag{2}$$

where $\{Z\}$ is a complex vector representing the sensor outputs and [F] is a matrix representing the displacement of the sensors for unit values of the generalized coordinates. The matrix [F] defines the sensor locations and ideally selects or isolates out only those generalized coordinates in the flutter analysis that are important to the flutter suppression system design. Since the number of sensors required in the flutter suppression system are in practice much less than the number of generalized coordinates, the matrix [F] will be singular and the more practical control law expressible in the form

$$\{\delta\} = [\bar{C}_R + i\bar{C}_I]\ \{Z\} \tag{3}$$

or

$$\{\delta\} = [\bar{C}_R + i\bar{C}_I]\ [F]\ \{q\} = [C'_R + iC'_I]\ \{q\} \tag{4}$$

This may be incorporated into the standard flutter equation as

$$[K]^{-1}\ \{[M] + [Q] + [Q_c]\ [C'_R + iC'_I]\}\ \{q\} = \frac{(1+ig)}{\omega^2}\ \{q\} \tag{5}$$

where [K] and [M] are the generalized stiffness and mass, respectively, of the structure; [Q], the generalized aerodynamic force matrix excluding the contribution of the active controls; and $[Q_c]$, the sum of the generalized aerodynamic forces and inertias due to the active control input. The flutter damping parameter g and flutter frequency ω make up the flutter eigenvalue. In the analytical design study, only M = 0, sea-level conditions were investigated since they represented the anticipated wind-tunnel conditions. Equation (5) was, therefore, solved initially by the standard V-g method employing a parameter optimization technique to determine the control coefficients that maximized the flutter speed for selected configurations of the AFFDL flutter model.

This procedure employed only one active aerodynamic control in the form of a stabilator or aileron control. In addition, the study investigated control

feedback systems employing feedback from all the generalized coordinates as well as from those that could be measured by employing only two and three motion sensors. These sensors were placed in an optimal manner over the model planform to sense the most significant modes contributing to the flutter instability of the model. Details on this analysis can also be found in reference 5.

The accuracy of the analytical modeling on the AFFDL flutter model is illustrated in figure 9 where the experimentally determined flutter speed from reference 2 is superimposed on this figure. The present analysis differs slightly from the computed AFFDL flutter results. This is thought to be due to the different input mode shape procedures followed in the present study. This study utilized basically an external localized least-squares fit to the modal data and input slopes and deflections directly at the one-quarter-chord and three-quarter-chord points of the aerodynamic boxes. This essentially bypassed the global least-squares fit routine in the standard program input format. A slight gain in computational accuracy is anticipated by this procedure. This is further confirmed in figure 10 for a slightly different sweep configuration. The math model is thought to accurately represent the flutter characteristics of the AFFDL wind-tunnel flutter model described in reference 2.

By employing a Nissim form of control law and parameter optimization techniques, a flutter suppression system evolved employing an active stabilator control that increased the system flutter speed above that of the isolated wing. This is illustrated in figures 11 and 12. As indicated in figure 11, this could be accomplished by employing only two motion sensors, one on the wing tip and a second on the tip of the stabilator. It is further indicated here that no significant difference would be obtained even if all the generalized coordinates were measured. Figure 13 illustrates that further gains in flutter margin could be achieved for this configuration if an active aileron control were employed in place of a stabilator. This aileron configuration is illustrated in figure 14. Flutter margins were again improved beyond that of the isolated wing even when employing the same aileron for active control of the isolated wing to gain additional flutter margin. Similar features were found for the 45° sweep configuration. All these preliminary studies were felt to be positive enough to warrant the design of an experimental wind-tunnel flutter program that would check the accuracy of the flutter suppression system design and lend a degree of confidence to the math modeling.

FINALIZED WIND-TUNNEL MODEL DESIGN

As mentioned earlier, the basic model employed in this study is a variation on the AFFDL wing-tail flutter model designed by the Air Force Flight Dynamics Laboratory and discussed in reference 2. Some of the model design details were modified by personnel at The University of Texas at Austin to include an active stabilator control in pitch and a remote control of the wing sweep angle. This model and its installation in the 7 ft by 10 ft wind tunnel at Wichita State University is illustrated in figure 15. The model degrees of freedom include a rigid body roll mode, wing root bending and torsional flexibilities, fuselage torsional flexibility, and fully flexible wing and stabilator modes. In addition, the stabilator could be remotely pitched by means of a

hydraulic actuator to provide a stiff control degree of freedom. The wing could also be remotely swept with a hydraulic actuator to simulate various geometries as well as rapidly convert the flutter model to a stable configuration by quickly sweeping the wing forward, raising the system's flutter speed. This latter feature was added with the hope that in some cases it could suppress undesirable model responses that may occur during critical flutter conditions.

A schematic of the model's hydraulic control supply system, employed to activate both wing sweep and stabilator motions, is illustrated in figure 16. This control system is comprised of three major assemblies: the hydraulic power supply module, the servo control module, and the model hydraulic actuator system designated respectively as (a), (b), and (c) in the schematic. These components are also illustrated in figure 17. The hydraulic power supply module is built around an Everpac Model PA-101 air driven hydraulic pump obtained without charge from government surplus. The pump provides a flow of 7.647 cm^3/sec (0.467 in^3/sec) at 690 N/cm^2 (1000 psi) which is the normal working pressure of the system. Due to the relatively small capacity of the self-contained reservoir within the pump, an additional reservoir was installed in the hydraulic return line. The hydraulic power supply module also provides, to both the wing sweep system and the stabilator sweep system, backup accumulators charged to 345 N/cm^2 (500 psi) with nitrogen. These accumulators further serve to attenuate fluctuations in line pressure caused by pulsations of the pump or head pressure.

The servo control modules are mounted atop and outside the wind tunnel next to the model to minimize line lag effects to the model control actuators. This module provides terminal points for the servovalve electronics and houses two surplus Moog Model 971A servovalves rated at 18.03 cm^3/sec (1.1 in^3/sec) at 8 mA. These servovalves are employed to activate two Clippard Minimatic 7DD-1 double-acting actuators driving the wing sweep and stabilator motions. One end of the actuator rods is attached to a linear variable differential transformer (LVDT) which provides for precise control of the stabilator pitch and wing sweep angle while the other end drives the linkage motion. Signals to the wing sweep servoamplifier include the wing sweep control signal, position feedback from the wing sweep LVDT, and a dither signal to keep the valve free of sediment and improve transient response. Signals to the stabilator pitch servoamplifier include the conditioned transducer signals, position feedback from the stabilator pitch LVDT, and the dither signal.

The control feedback avionics, developed as a part of the flutter suppression system, are illustrated in figure 18. An analog control was developed due to the expense and complexity of digital systems. The avionics for the stabilator pitch control include printed circuit modules for input control and amplification, integration, and phase shifting. It allows for up to three channels of output which can command up to three separate aerodynamic surfaces. The unit can monitor signals from accelerometers, velocity pickups, and/or strain gages mounted at select positions on the model and blend these according to a preselected control law. The modular grouping of the different circuits in this manner permits the programing of a variety of control laws.

Chains of inexpensive high-input impedance operational amplifiers, which

constitute the basic elements of analog computers, were put together to perform the required control functions. EGC 941 M op amps were first breadboarded into functional blocks and tested to determine component values for best performance. Continuing the concept of functional blocks, modular construction was adopted in the layout of the model control panel thus enabling quick replacement of defective circuits and testing on a modular basis. Other benefits of modular construction were realized including ease in circuit modification and construction, as well as circuit substitution if desired. This system's approach to circuit design is discussed in reference 6 and greatly extends the capabilities of the design engineer who is faced with problems in the active control technology area.

VIBRATION AND FLUTTER STUDIES

In an attempt to obtain the most accurate math modeling for the study, experimental inputs were utilized in the analysis whenever practical. This included measurements of vibration modes, frequencies, and generalized masses for the first five modes of the system. Table I illustrates a comparison of the first five modal frequencies measured on the present model at a 60° sweep configuration with one of the models described in reference 2. Attempts were also made to measure the model's first five generalized masses following the procedures outlined in reference 7. The results of this study are illustrated in figure 19. An alternate study is currently in progress to make direct mass measurements that can hopefully be correlated with these data. The generalized mass data appear reasonable except possibly for the third mode which was difficult to excite in a clean responsive manner. Further studies are in progress to completely define the structural dynamic characteristics of the model as accurately as practical for several sweep configurations.

By mid-December 1974 the basic model design and fabrication had been completed to the point that an uncontrolled two-day flutter test was possible. These initial tests were conducted at the Walter H. Beech Memorial Wind Tunnel on the campus of Wichita State University, Wichita, Kansas. The test program provided basically a checkout of the model instrumentation and structural integrity in addition to a flutter data point that could be correlated with the computed flutter point provided by our math model. The uncontrolled model fluttered spontaneously at 70 meters per second (230 ft/sec) at a frequency of 8 Hz in the classical wing-tail flutter mode, whereas the model of reference 2 had a flutter speed of approximately 39 meters per second (230 ft/sec). Flutter was suppressed without damage to the model by a reduction of dynamic pressure in the wind tunnel. These results confirmed that the frequency range of unstable model responses lies well within the 0 to 15 Hz levels for which satisfactory preliminary checkouts have been made on the model control system. Finalized checkouts are currently being made on the model's overall control response characteristics to define completely the control transfer function.

CONCLUDING REMARKS

The preliminary findings obtained from the current study indicate that an active aerodynamic control in the form of a stabilator or aileron can be highly effective in suppressing subsonic wing-tail interference flutter. Flutter margins can be restored to at least that of the isolated wing by employing control gains and phasings utilizing parameter optimization techniques. The doublet lattice lifting surface theory was found to be adequate for predicting this flutter phenomenon as observed in the wind tunnel. Additional wind-tunnel studies are needed on the modified AFFDL wing-tail flutter model, however, to accurately assess the math modeling techniques employed in the present study for designing flutter suppression systems. One such test program is planned for the near future. Preliminary wind-tunnel studies have been carried out on the uncontrolled flutter model developed in the present study. The results verified the structural integrity of the model for the more advanced testing programs and provided a checkout of the instrumentation and a data point for correlation with our math model. Recent electronic developments in the form of both analog and digital modular devices at extremely low costs have brought many of the problem solutions in the active control technology area to within both the technical and economical grasp of the academic researcher as well as the alert designer.

REFERENCES

1. Topp, L.J., Rowe, W.S., and Shattuck, A.W.: Aeroelastic Considerations in the Design of Variable Sweep Wing Airplanes. ICAS/RAES, Sept. 1966, pp.1-25.

2. Mykytow, W.J., Noll, T.E., Huttsell, L.J., and Shirk, M.H.: Investigations Concerning the Coupled Wing-Fuselage-Tail Flutter Phenomenon. Journal of Aircraft, Vol. 9, No. 1, Jan. 1972, pp. 48-54.

3. Shelton, J.D., Tucker, P.D., and Davis, J.C.: Wing-Tail Interaction Flutter of Moderately Spaced Tandem Airfoils. AIAA Paper No. 69-57, AIAA 7th Aerospace Sciences Meeting, New York, Jan. 20, 1969.

4. Nissim, E.: Flutter Suppression Using Active Controls Based on the Concept of Aerodynamic Energy. NASA TN D-6199, 1971.

5. Cwach, E., and Stearman, R.: Suppression of Flutter on Interfering Lifting Surfaces by the Use of Active Controls. AIAA Paper No. 74-404, AIAA/ASME/SAE 15th Structures, Structural Dynamics and Materials Conference, April 17-19, 1974.

6. Sheingold, D.H.: Nonlinear Circuits Handbook. Analogue Devices Inc., Norwood, Massachusetts, 1974.

7. Able, I.: A Wind Tunnel Evaluation of Analytical Techniques for Predicting Static Stability and Control Characteristics of Flexible Aircraft. NASA TN D-6656, 1972.

TABLE I

MODAL FREQUENCIES
60° SWEEP CONFIGURATIONS

MODE NUMBER	AFFDL MODEL REF. 2 Hz	MODIFIED AFFDL MODEL PRESENT STUDY Hz
1	0.90	1.46
2	3.9	3.82
3	8.1	7.89
4	13.9	16.93
5	17.1	21.90

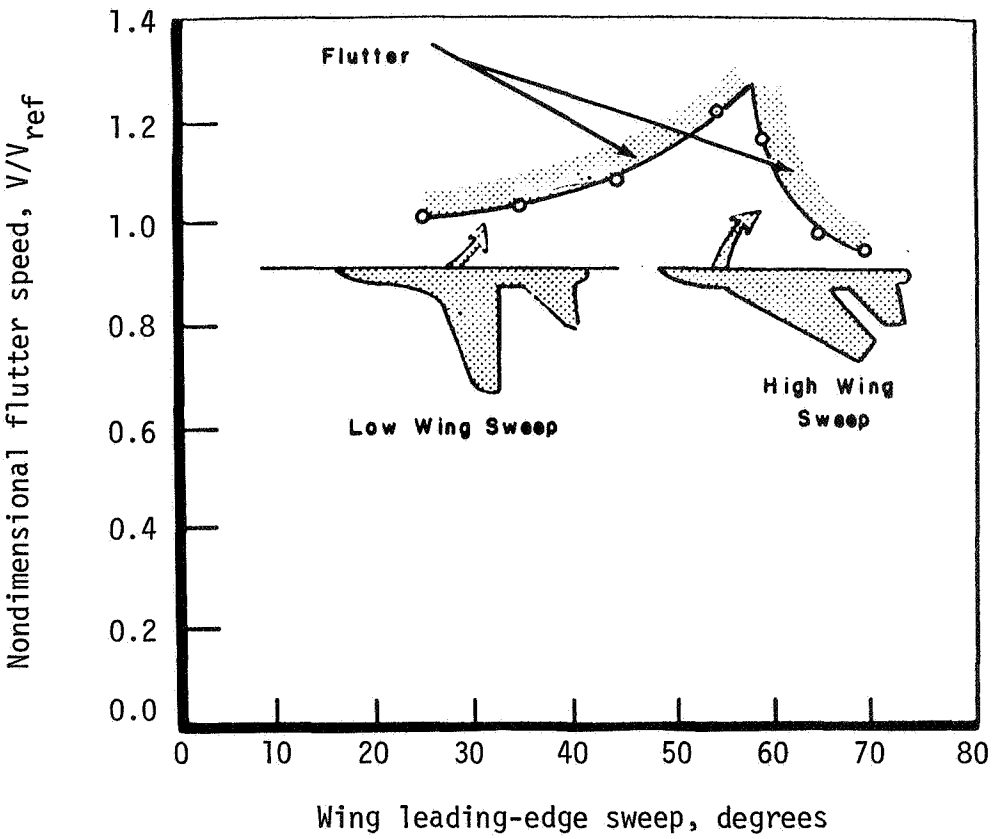

Figure 1.- Composite flutter boundary illustrating critical interference flutter condition for large sweep angles. (From reference 1.)

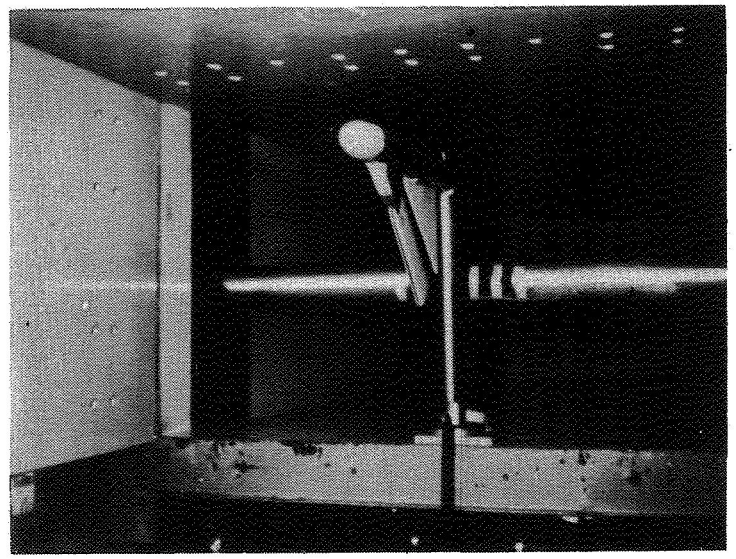

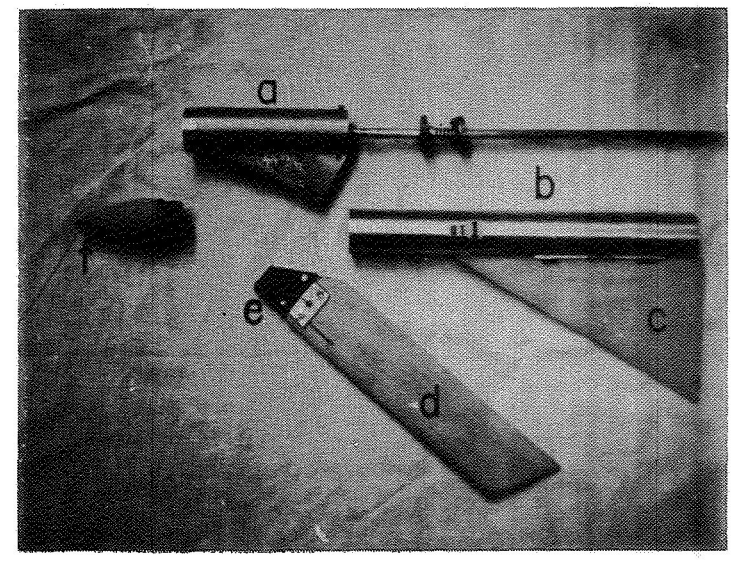

Figure 2.- Semirigid wing-tail flutter model. Construction details and installation in 3 ft by 4 ft wind tunnel.

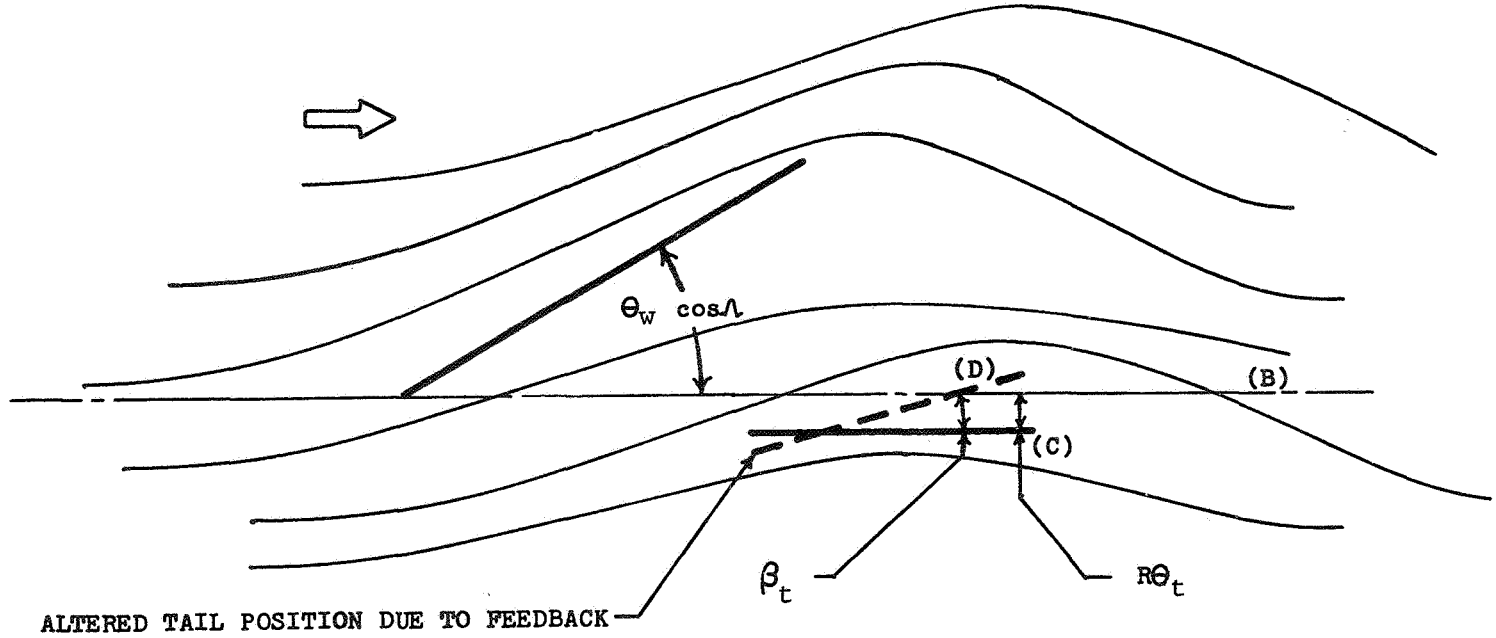

Λ = Wing sweep angle
R = Distance from central axis to typical section
θ_w = Wing flap angle
θ_t = Tail flap angle
β_t = Stabilator pitch angle

Figure 3.- Typical section flow field for wing-tail flutter model.

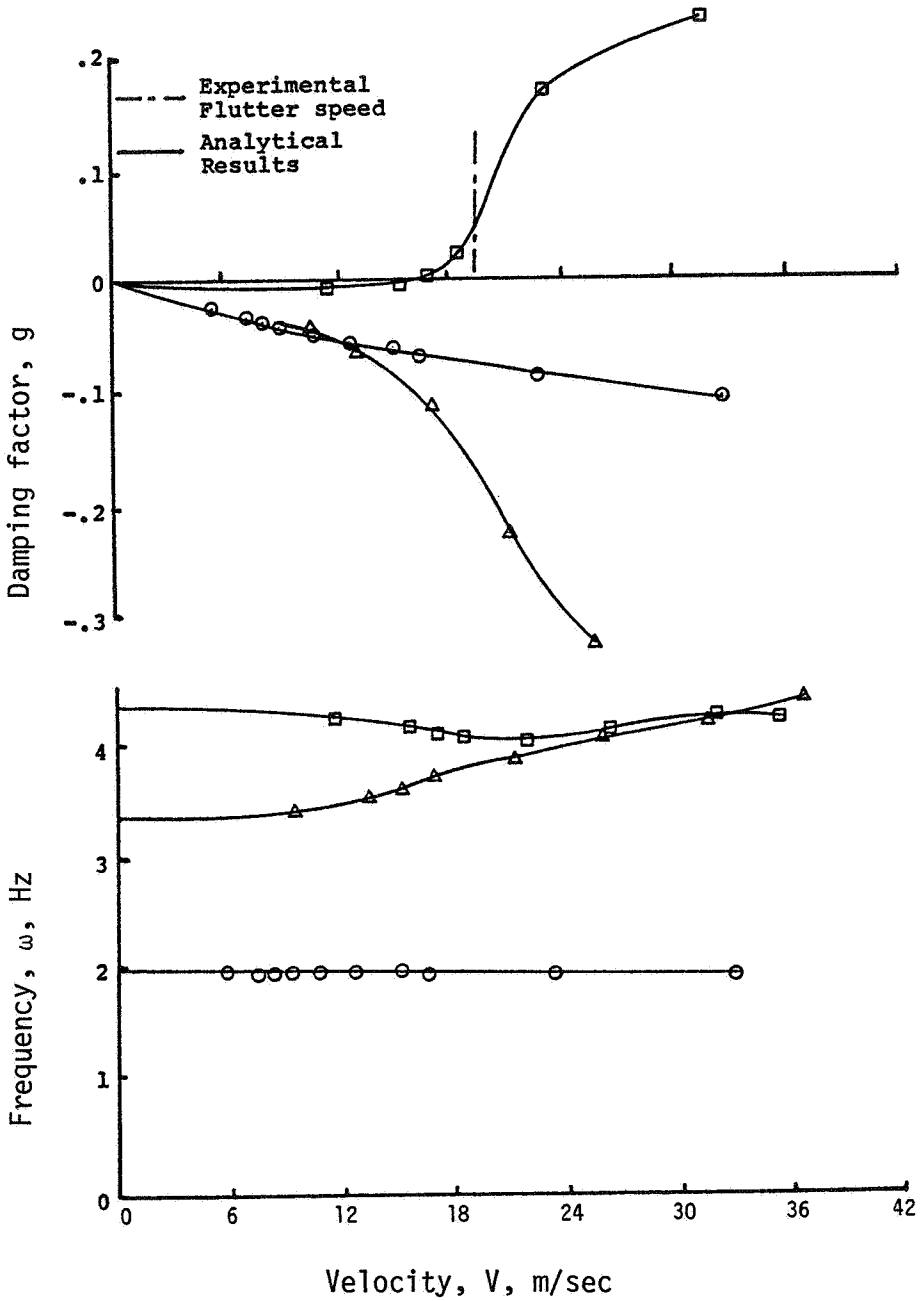

Figure 4.- Semirigid wing-tail model. Uncontrolled flutter speeds (open loop). 60° sweep configuration and approximately 1/4 wing chord separation distance between wing and tail; M = 0; sea-level conditions.

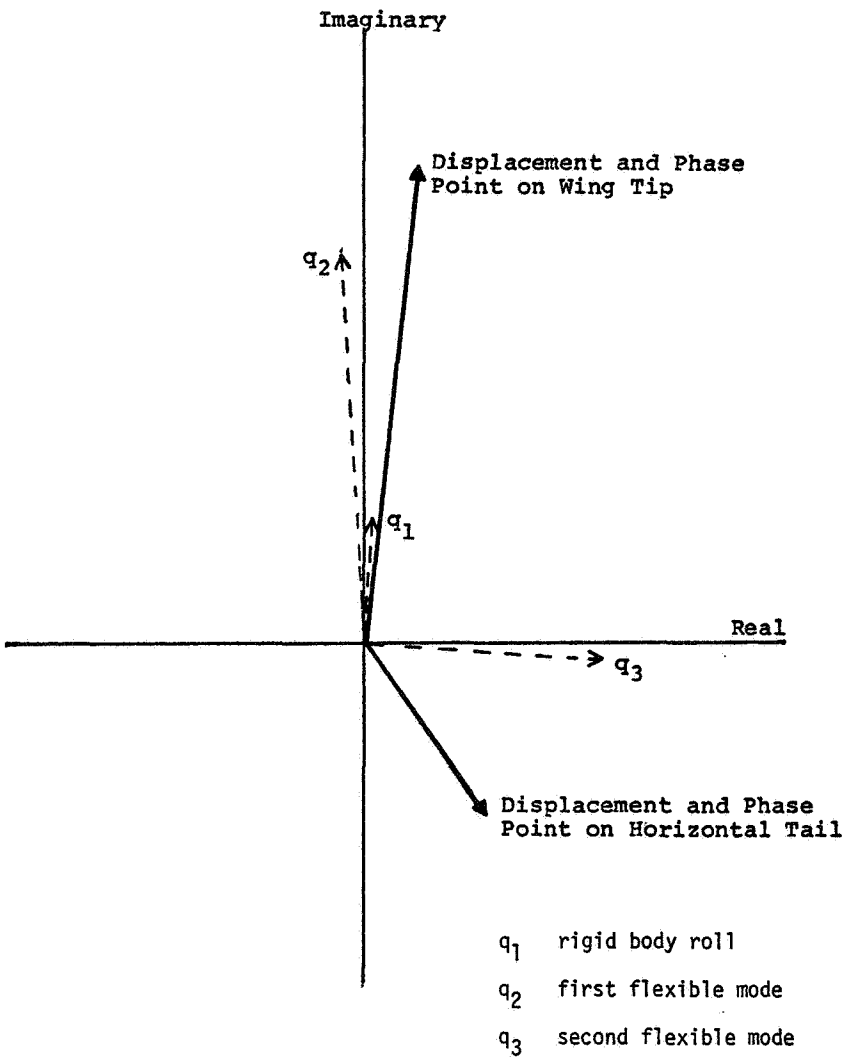

Figure 5.- Computed displacement and phase relationships in open loop flutter mode of semirigid wing-tail model. 60° sweep configuration and approximately a 1/4 wing chord separation distance between wing and tail; M = 0; sea-level conditions.

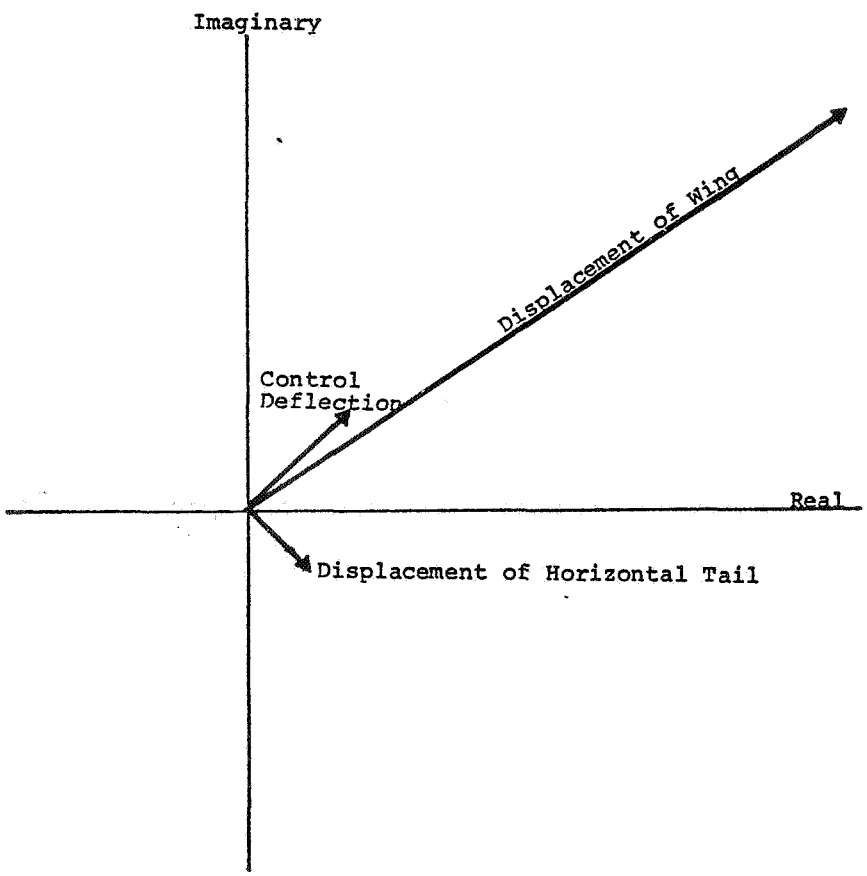

Figure 6.- Computed phase relationships between wing, tail, and control surface for controlled semirigid wing-tail model (sensor located on horizontal tail). 60° sweep configuration and approximately a 1/4 wing chord separation distance between wing and tail; M = 0; sea-level conditions.

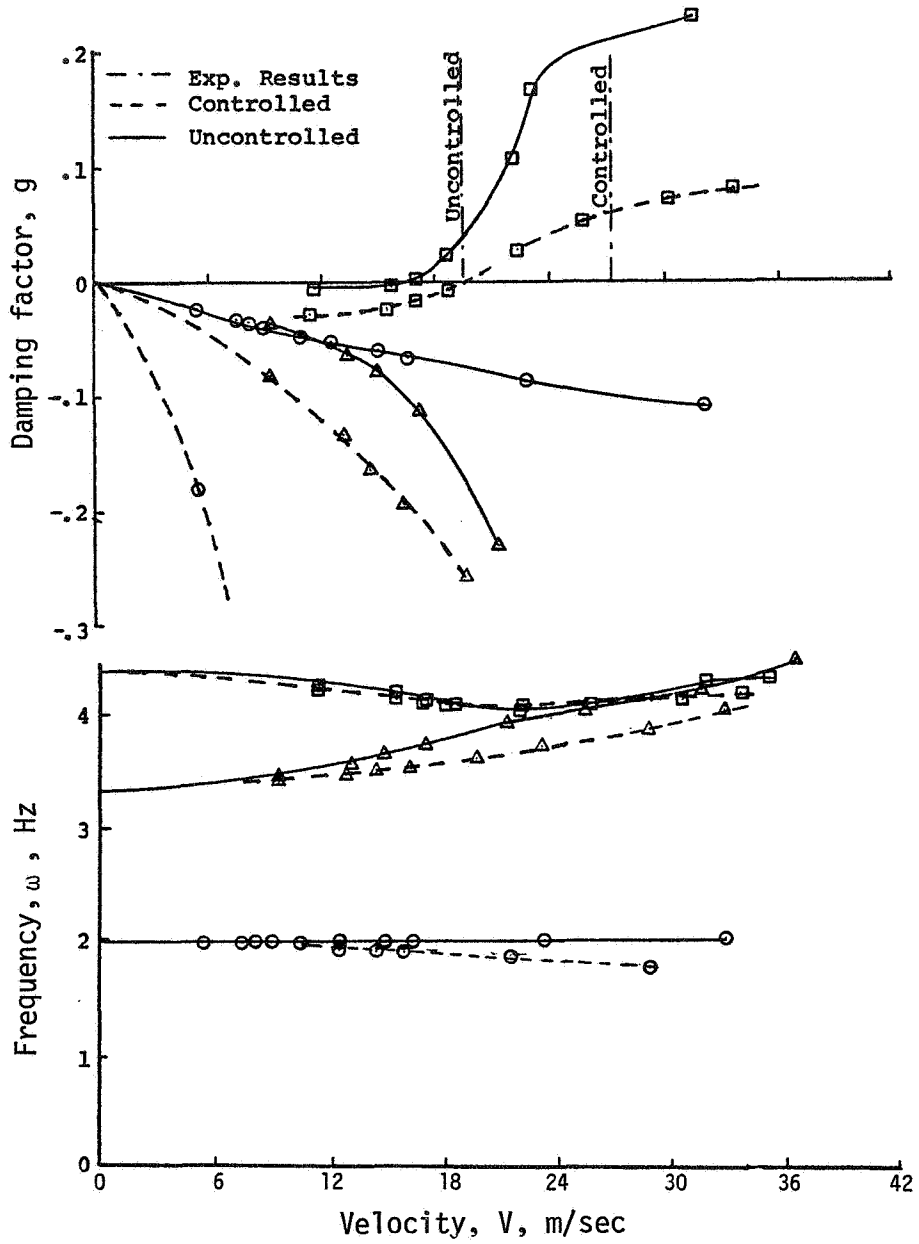

Figure 7.- Semirigid wing-tail model controlled and uncontrolled flutter speeds (experimental and computed). 60° sweep configuration and approximately a 1/4 wing chord separation distance between wing and tail; M = 0; sea-level conditions.

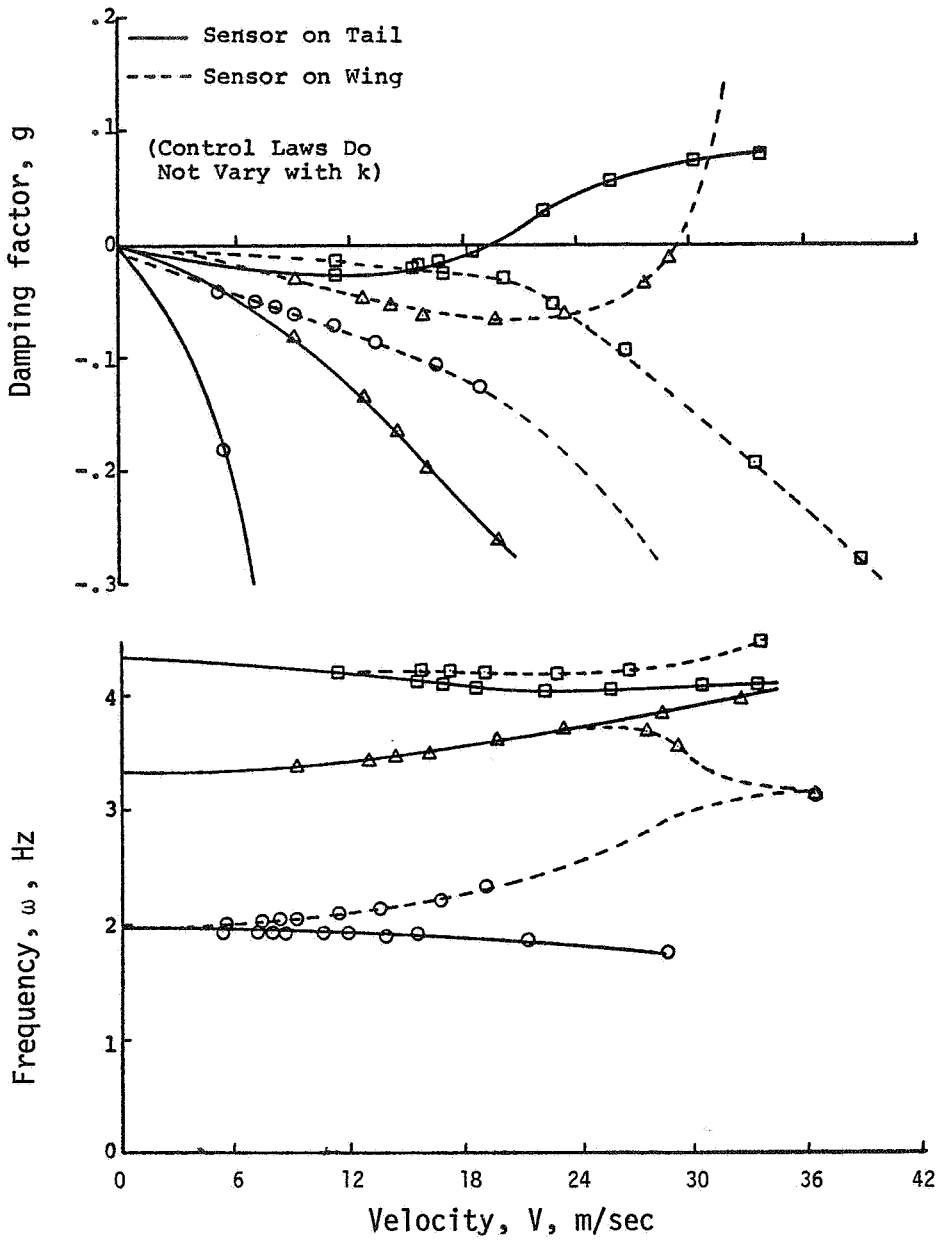

Figure 8.- Comparison of semirigid controlled model flutter results with sensor mounted on tail and wing.
M = 0; sea-level conditions.

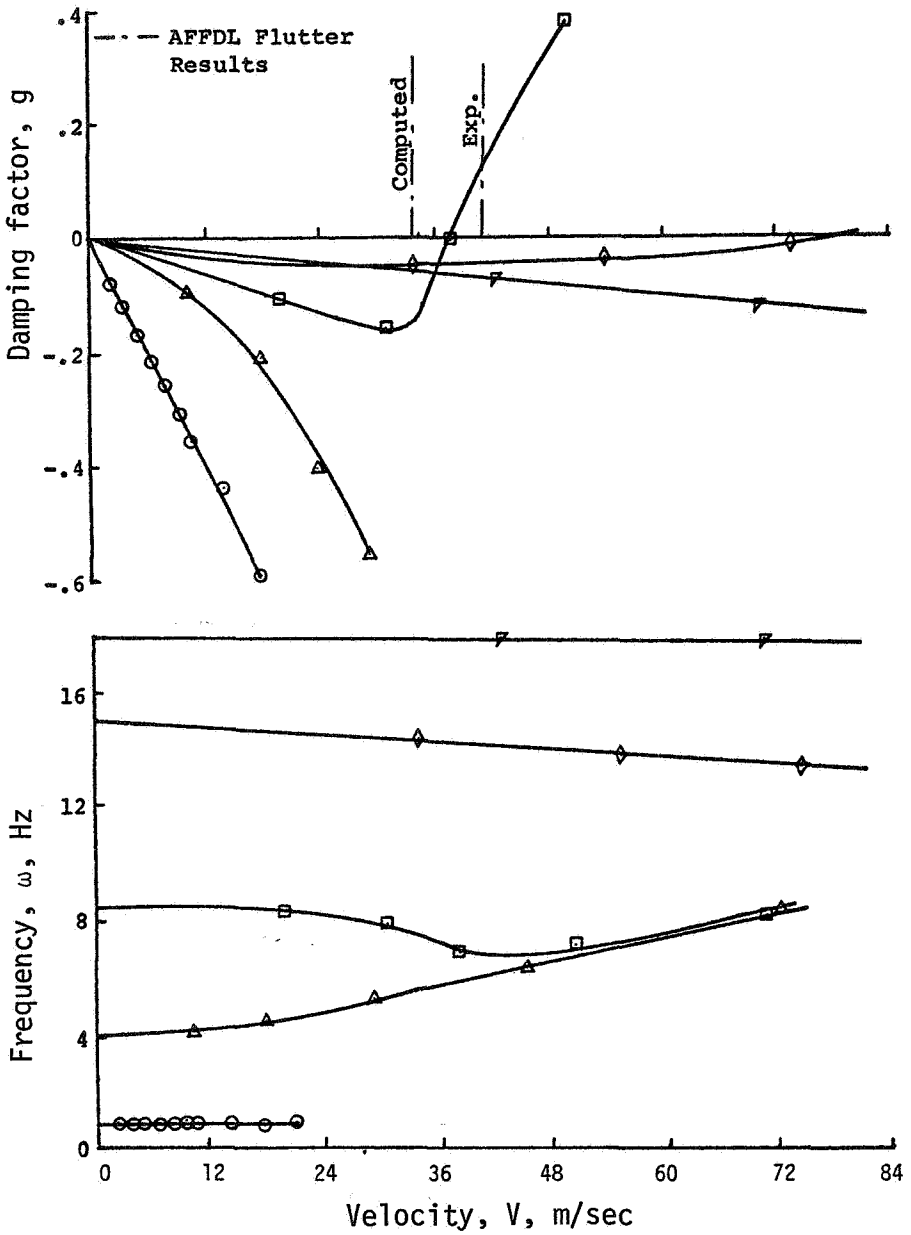

Figure 9. AFFDL model. Uncontrolled flutter speed; 60° wing sweep; M = 0; sea-level conditions.

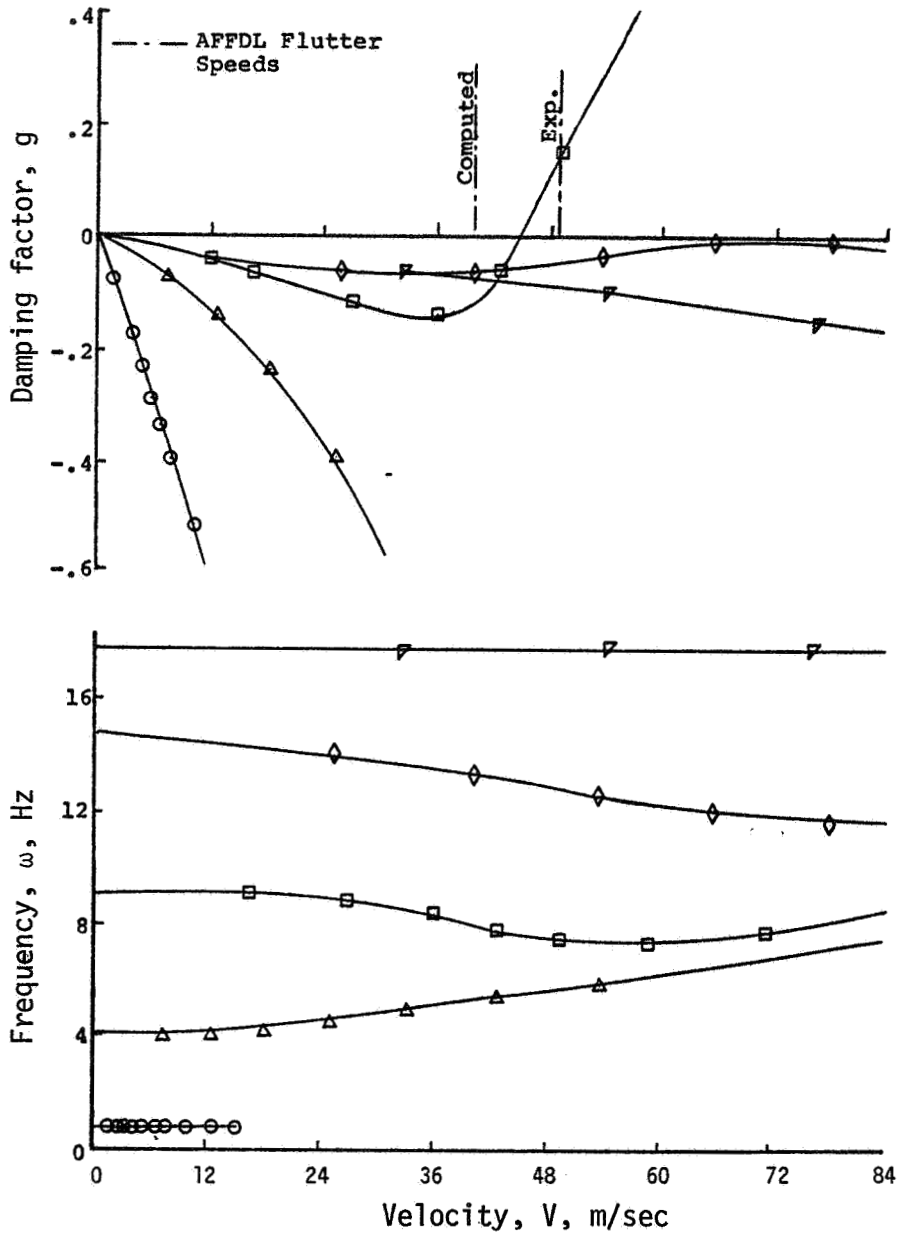

Figure 10. AFFDL model. Uncontrolled flutter speed; 45° wing sweep; M = 0; sea-level conditions.

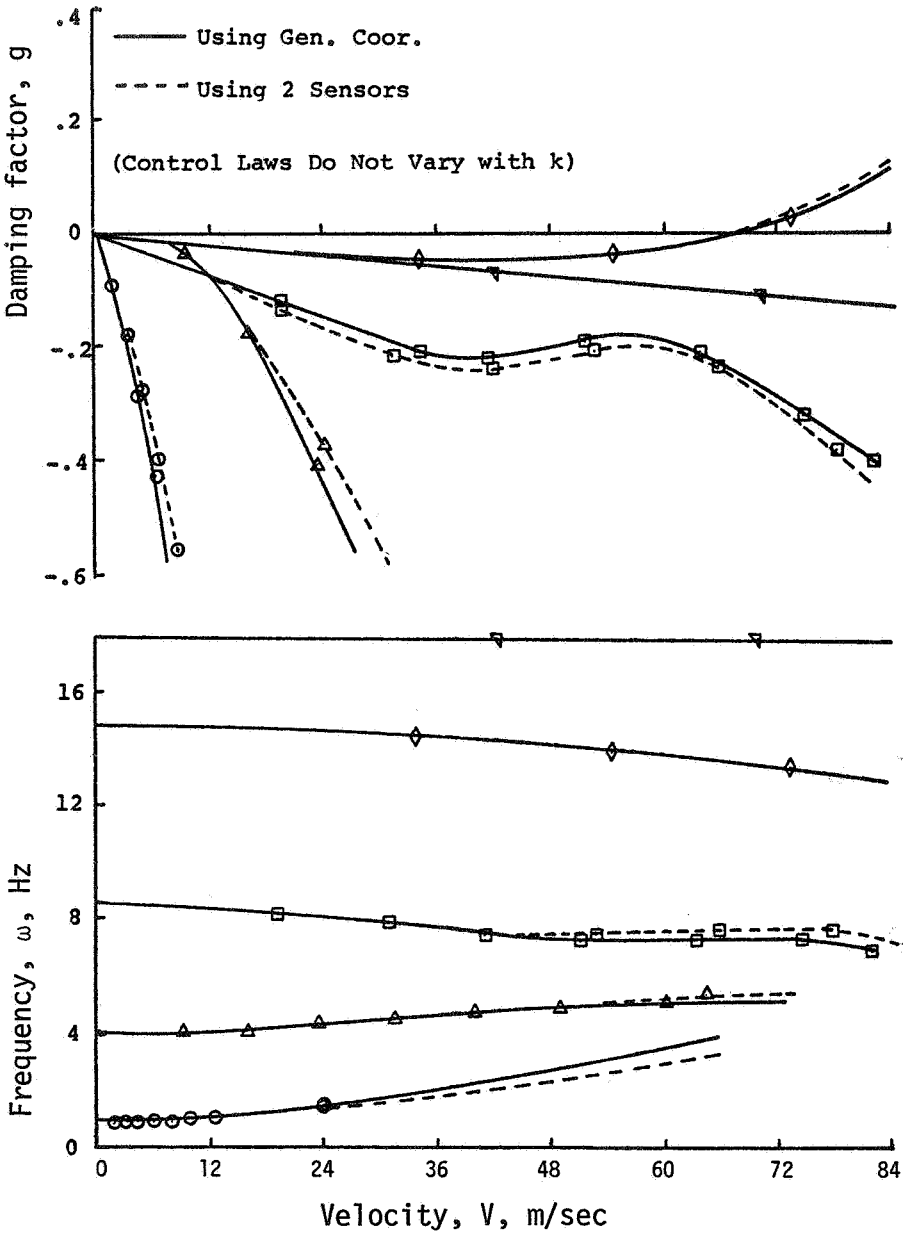

Figure 11. Comparison of flutter speeds on AFFDL model when using generalized coordinates and two sensors in control law (one sensor located near the outer wing tip trailing edge and one near the stabilator tip leading edge). 60° sweep configuration; active stabilator control; M = 0; sea-level conditions.

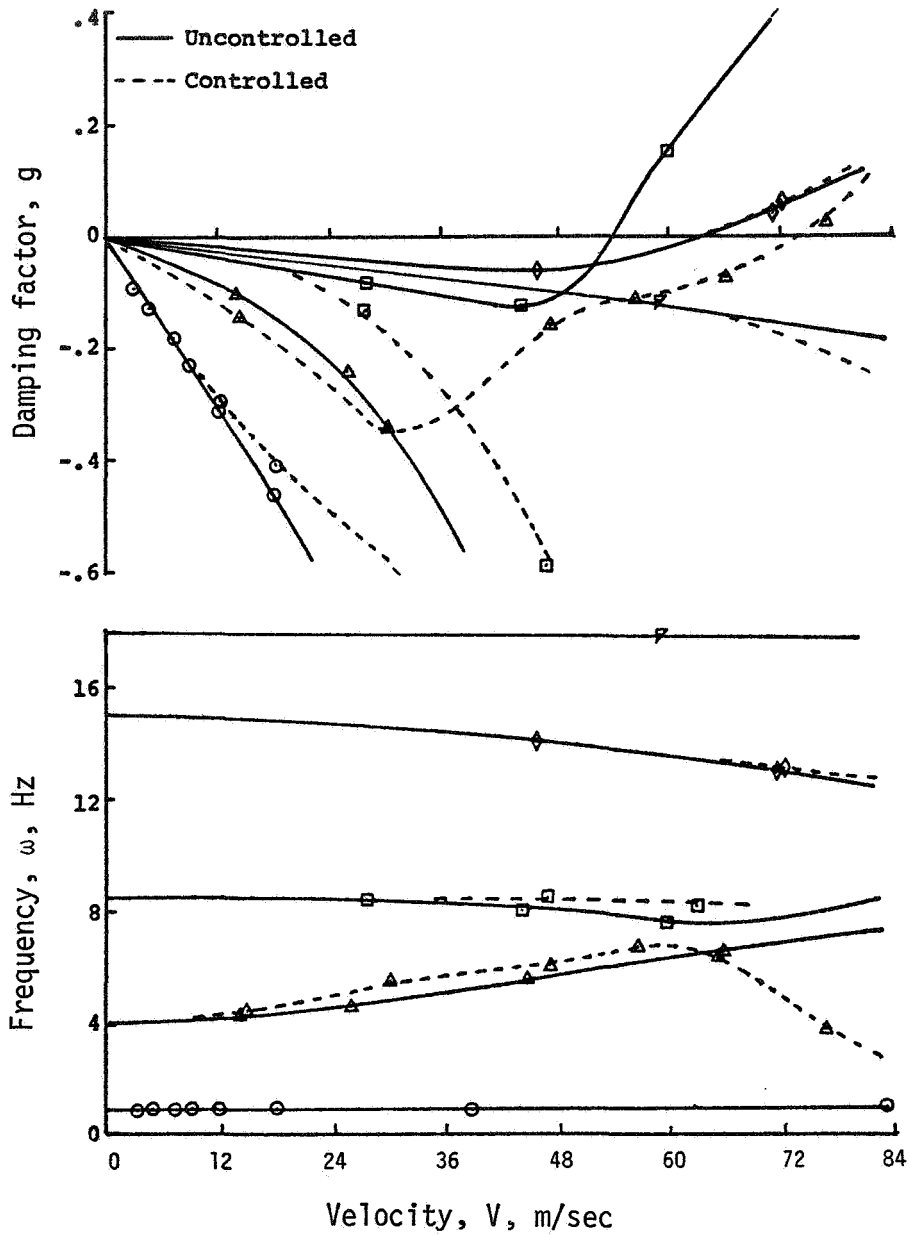

Figure 12.- Increase in flutter speed of isolated wing of AFFDL model. 60° sweep configuration; aileron is active control using generalized coordinates in control law; M = 0; sea-level conditions.

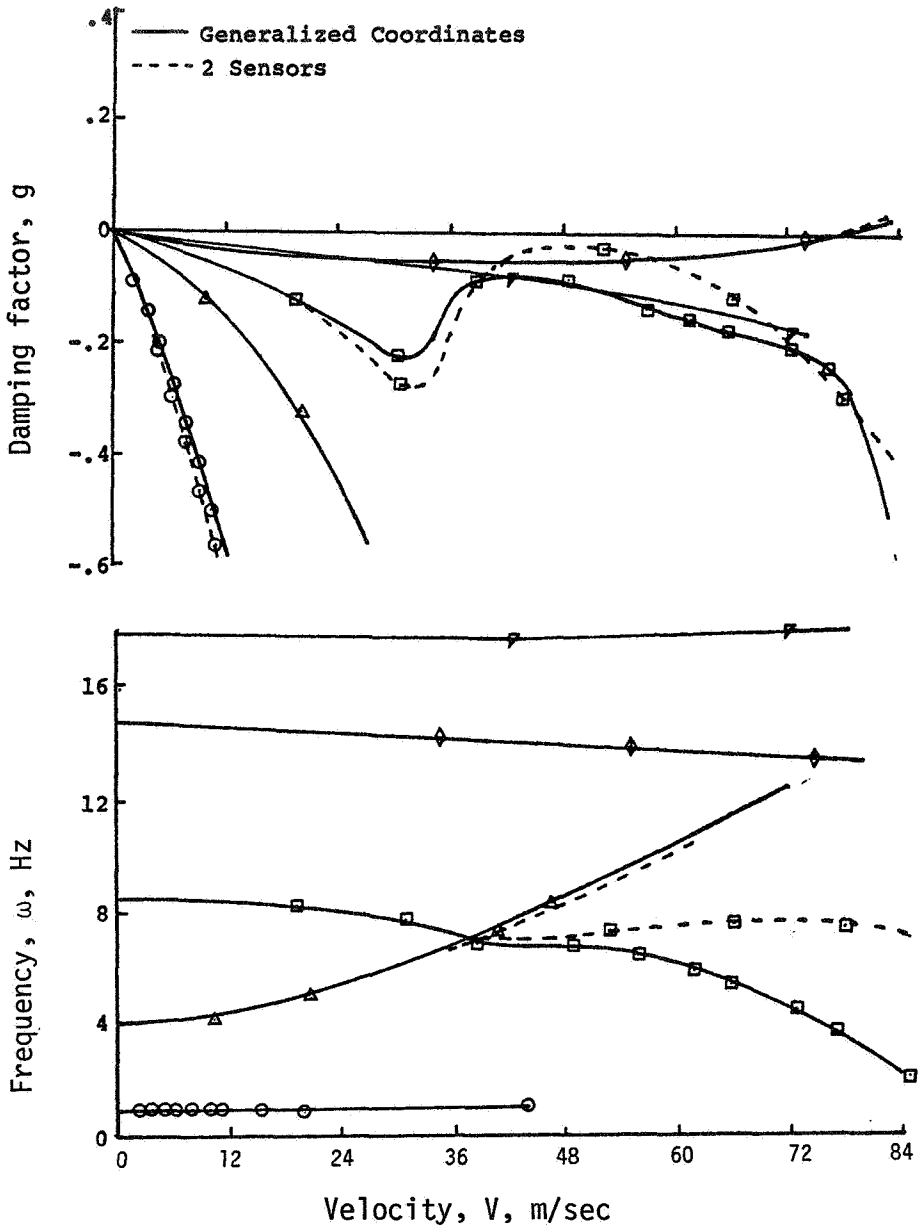

Figure 13.- Comparison of flutter speeds of AFFDL model using generalized coordinates and two sensors in control law (both sensors located on wing at 35% of local wing chord, one near the tio and one at the root chord). 60° sweep configuration; active aileron control; M = 0; sea-level conditions.

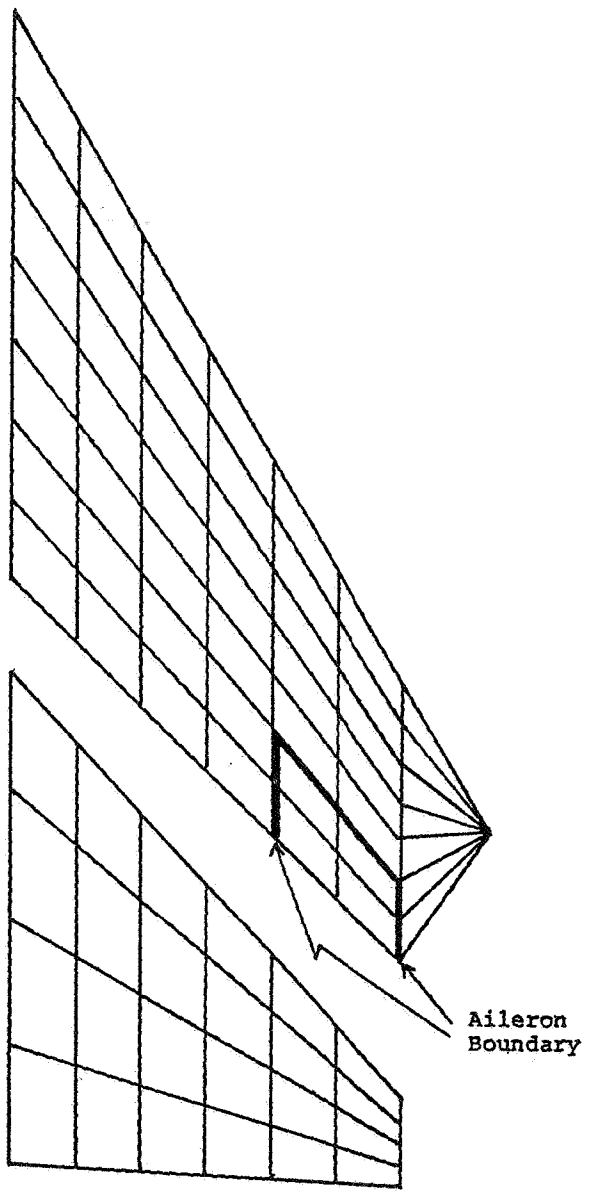

Figure 14.- Aerodynamic modeling for aileron on AFFDL model with 60° sweep.

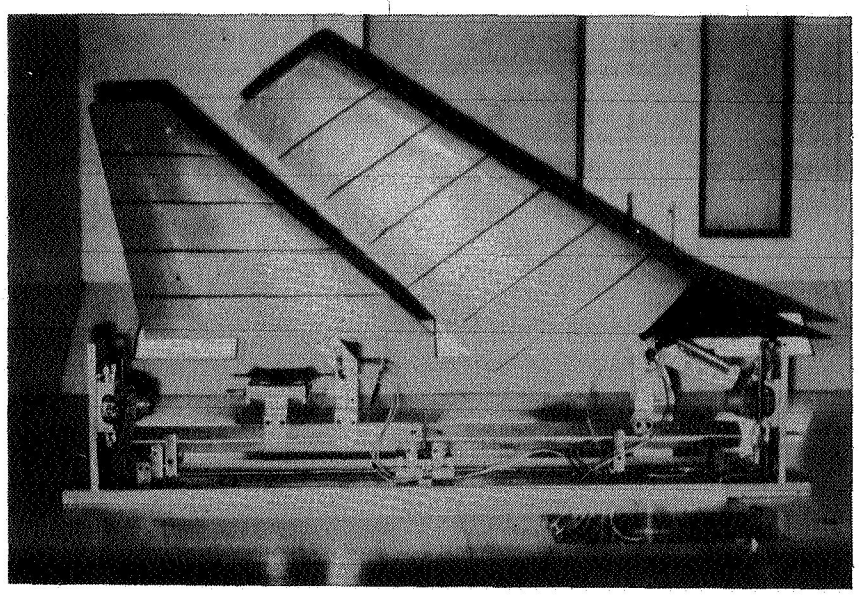

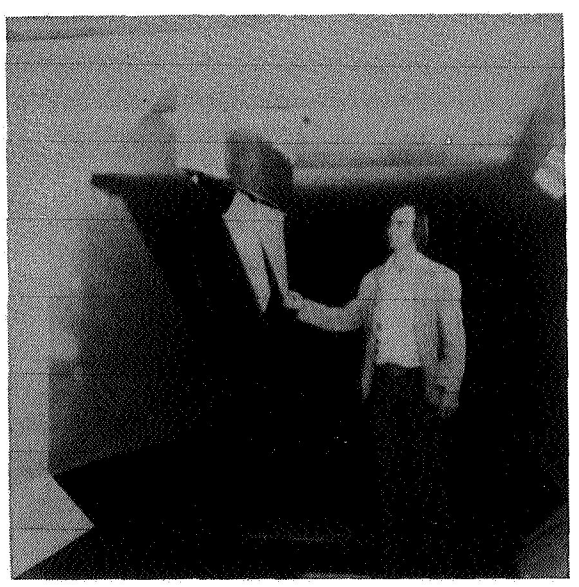

Figure 15.- Installation of modified AFFDL wing-tail flutter model in 7 ft by 10 ft subsonic wind tunnel.

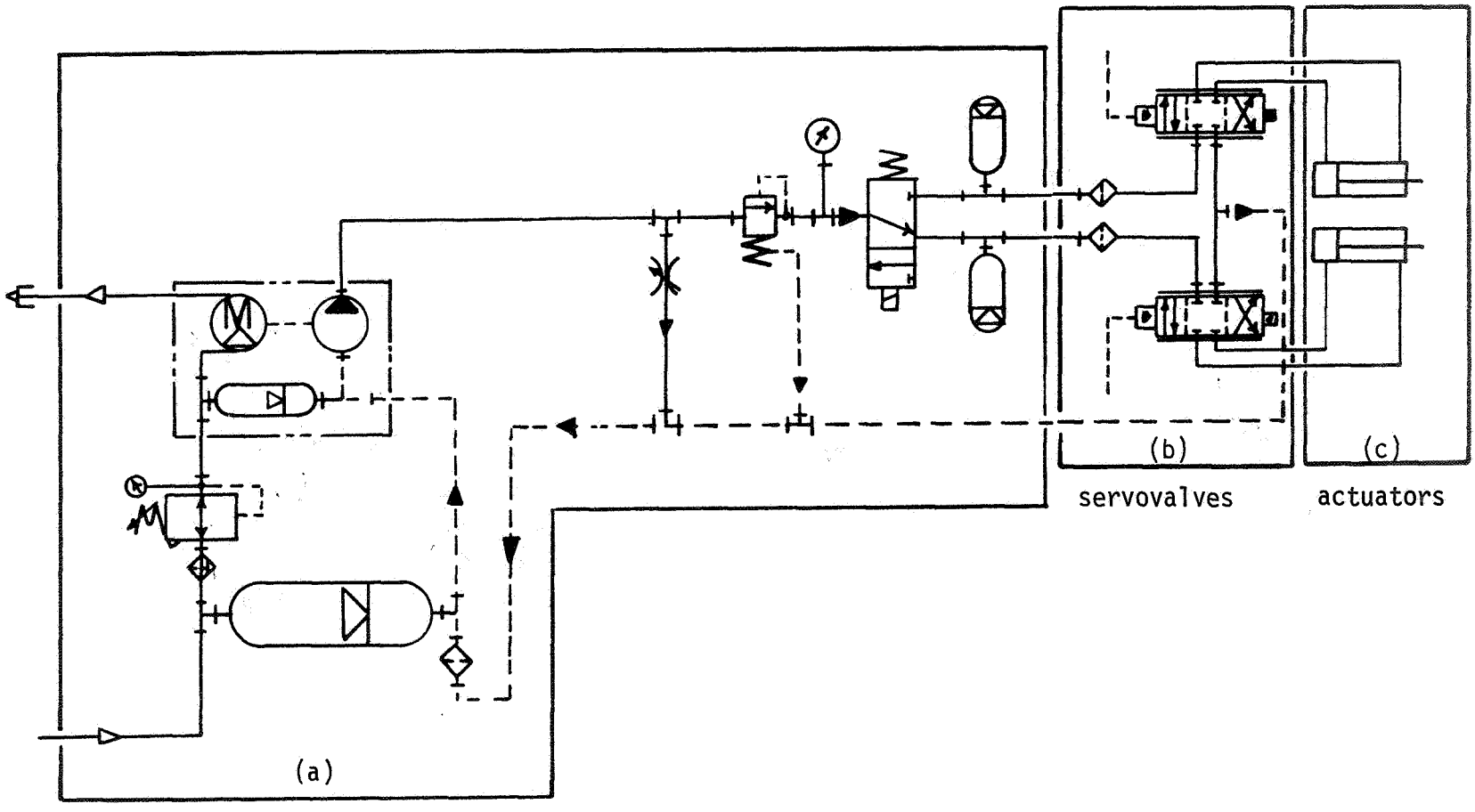

Figure 16. Schematic of hydraulic control systems for modified AFFDL wing-tail flutter model.

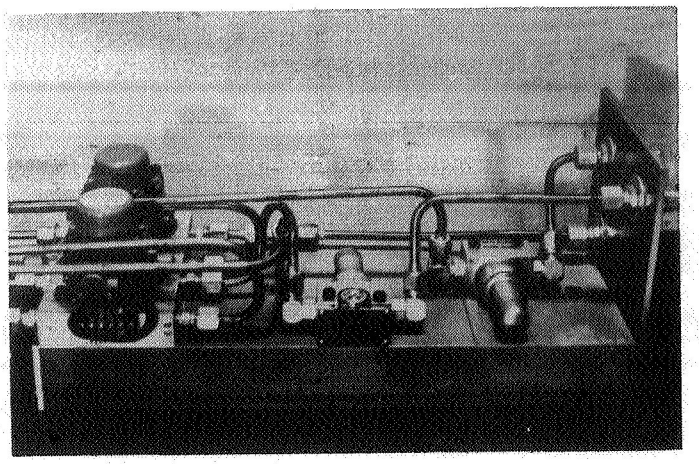

Servovalves

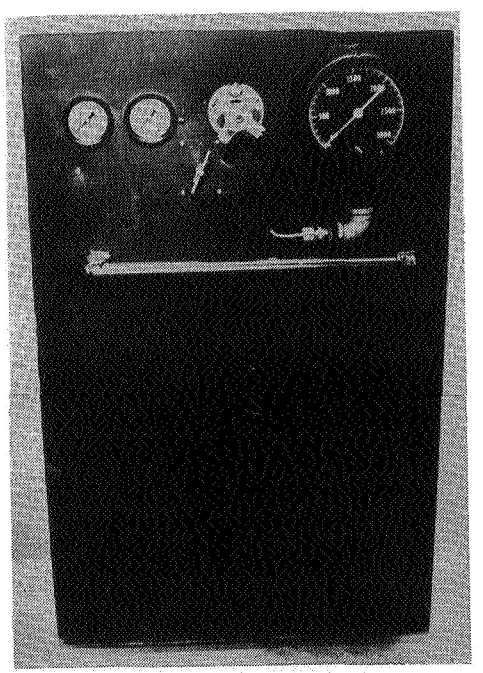

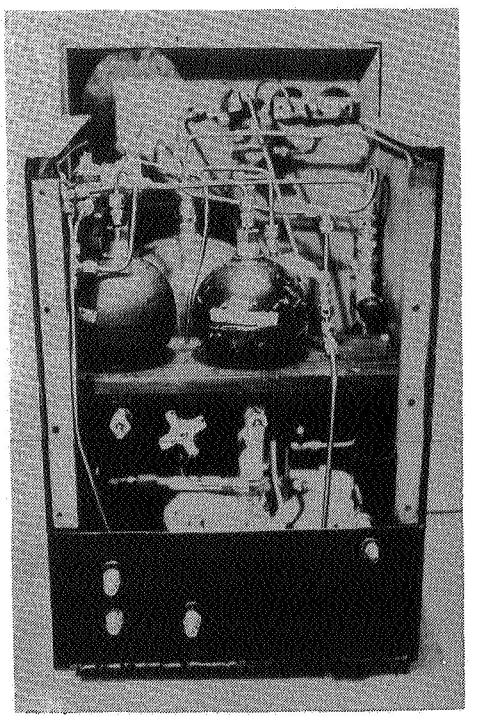

Hydraulic power supply

Figure 17.- Hydraulic power supply and servovalves for modified AFFDL wing-tail model.

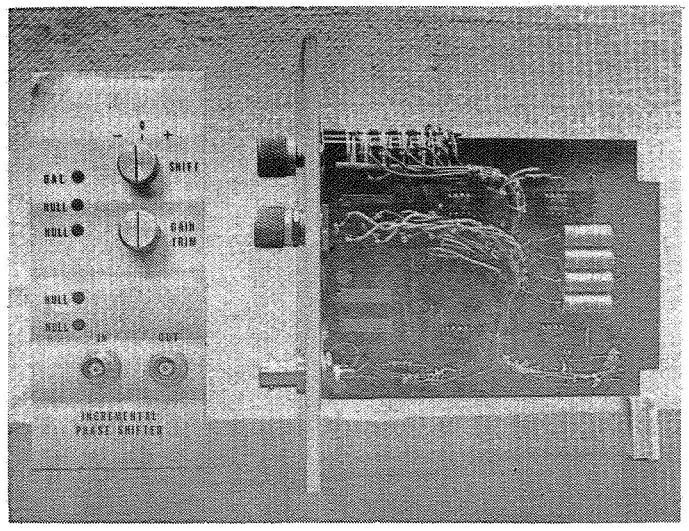

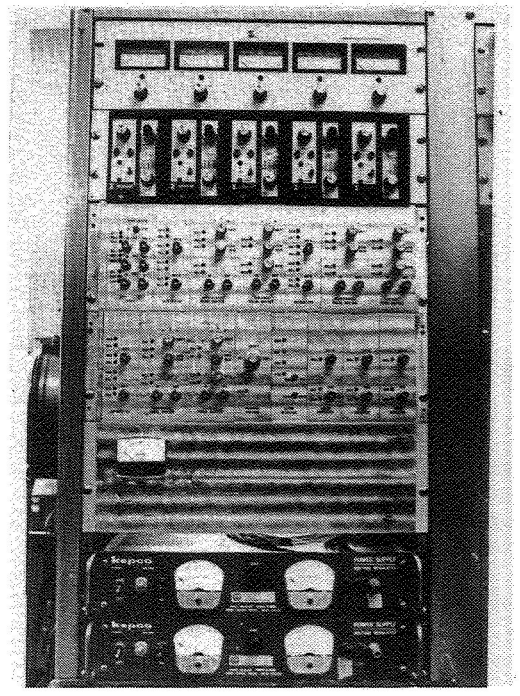

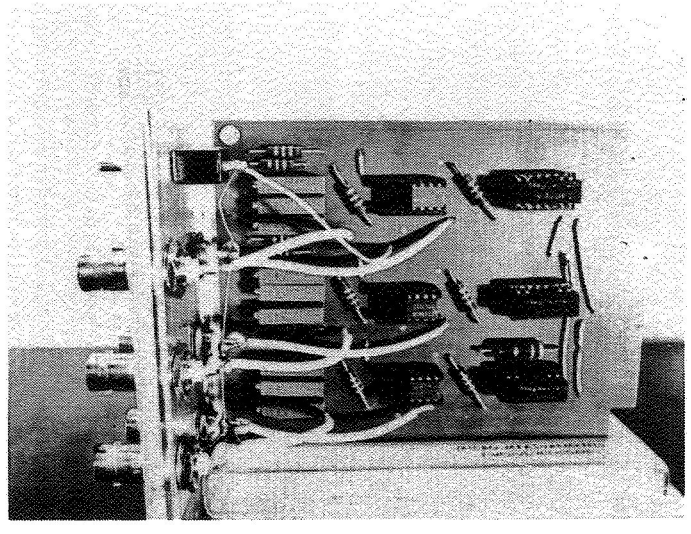

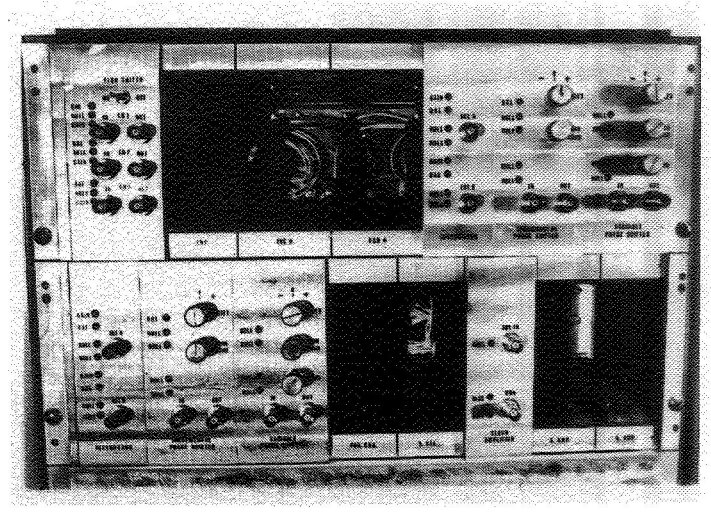

Figure 18.- Control feedback avionics for modified AFFDL wing-tail model. Small operational amplifiers illustrated along with modular units for performing various required control functions.

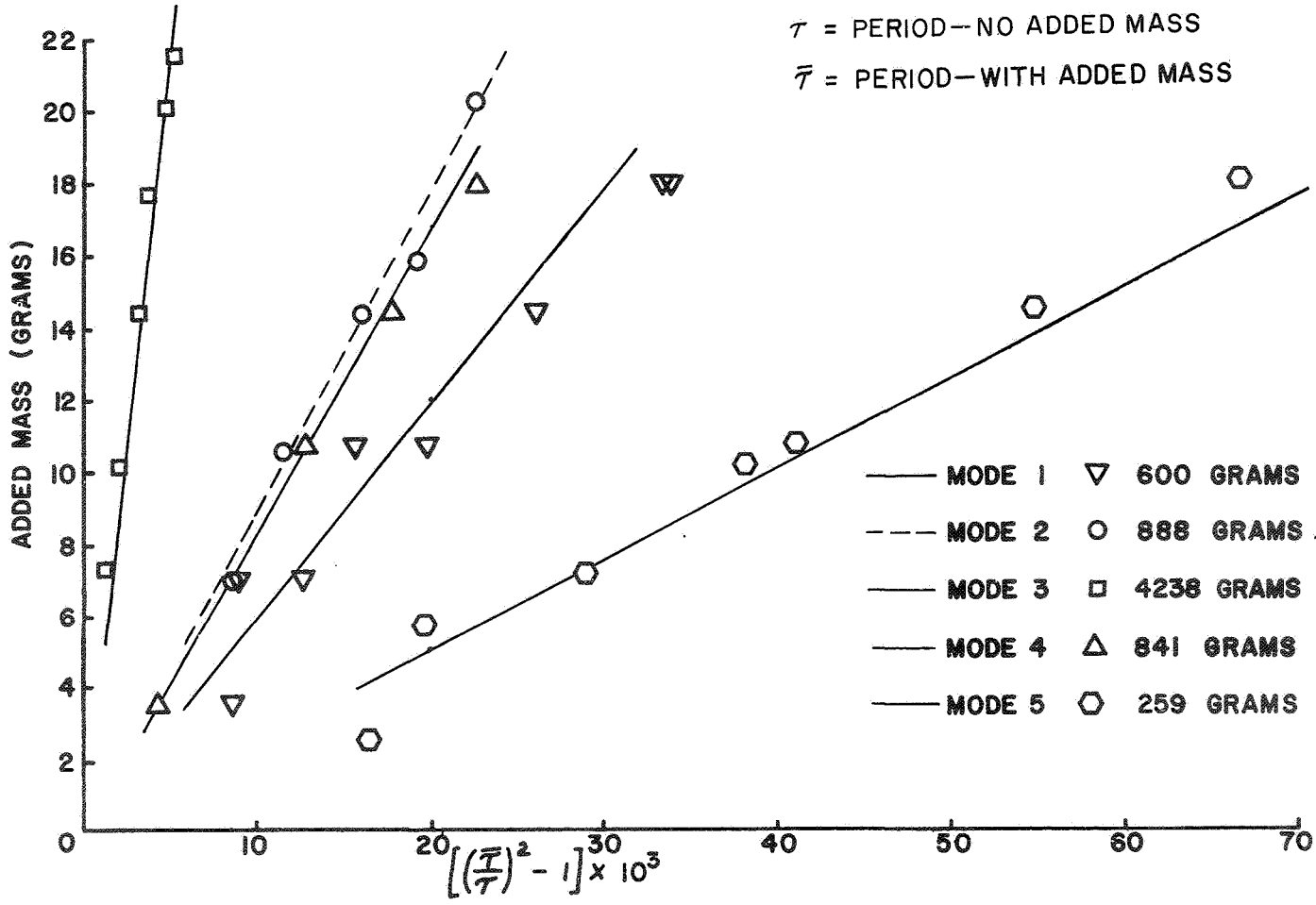

Figure 19.- Generalized mass measurements.